

Seasonal changes in sea ice conditions along the Northeast Passage in 2007 and 2012

Lei Ruibo^{1*}, Li Na¹, Li Chunhua² & Jónsdóttir Ingibjörg³

¹ Key Laboratory for Polar Science of the State Oceanic Administration, Polar Research Institute of China, Shanghai 200136, China;

² National Marine Environmental Forecasting Center, Beijing 100081, China;

³ Institute of Earth Sciences, University of Iceland, Reykjavik, 101, Iceland

Received 28 March 2014; accepted 15 September 2014

Abstract Remote sensing data from passive microwave and satellite-based altimeters, associated with the data measured underway, were used to characterize seasonal and spatial changes in sea ice conditions along the Arctic Northeast Passage (NEP) and the high-latitude sea route (HSR) north of the island groups in the eastern Arctic Ocean in 2007 and 2012. In both years, summer Arctic sea ice extent reached minima since satellite records began in 1979. However, there were large differences in spatial distribution of sea ice between the two years. Sea ice conditions in the eastern sections of the sea routes were relatively slight in the 2007 summer, because of the remarkable decline of sea ice in the Pacific sector. A belt of sea ice that blocked sections from the western Laptev Sea to the eastern Kara Sea resulted in both sea routes not completely opening through the 2007 summer. The combination of a great storm in early August causing sea ice to be sheared from the Arctic pack ice and the thick ice surviving the winter delayed the summer opening of the eastern parts of the sea routes in 2012. However, the average open period, defined by 50% ice concentration for the entire NEP and HSR, reached 82 d and 55 d, respectively. Thus, 2012 was the most accessible year since the satellite era began in 1979. The distinct decrease in sea ice in the western parts of the HSR in the 2012 summer can be attributed to the thinning preconditions of sea ice prior to the melt season. The HSR opening can benefit Arctic shipping of deeper-draft vessels.

Keywords sea ice, concentration, thickness, shipping, Arctic Northeast Passage

Citation: Lei R B, Li N, Li C H, et al. Seasonal changes in sea ice conditions along the Northeast Passage in 2007 and 2012. *Adv Polar Sci*, 2014, 25: 300-309, doi:10.13679/j.advps.2014.4.00300

1 Introduction

The Arctic Northeast Passage (NEP) is traditionally defined as a series of sea routes from northwest Europe around North Cape (Norway), and along the north coast of Eurasia and Siberia, through the Bering Strait to the Pacific^[1]. Shipping through the NEP reduces the distance between the Far East and Europe by 30%–40%, compared with the “Royal Road” via the Strait of Malacca and the Suez Canal. There is a long history of shipping in the NEP, dating back to the 17th

century^[1]. Recently, sailing routes through the passage have widened because of the decline in Arctic sea ice. Since the first trans-Arctic navigation through the NEP by a merchant vessel in the 2009 summer, the number of merchant vessels using this sea route has increased. This increasing economic viability of the NEP is exemplified by the 46 voyages carrying 1.26 million tons of cargo using this route during 2012^[2]. In August 2013, a Chinese merchant vessel, *Yongsheng*, departed from Dalian, China and sailed through the NEP toward its destination of Rotterdam, Netherlands. This was the first attempt by the world’s biggest exporter to

* Corresponding author (email: leiruibo@pric.org.cn)

exploit the Arctic sea route to reach its largest market: the European Union.

Both the extent and thickness of Arctic sea ice have decreased significantly in recent decades. In September 2007, Arctic sea ice extent reached the minimum recorded in the satellite era began in 1979, and in September 2012 this record was broken again. In 2012, the extent of sea ice in September was reduced by 45% compared with the 1981–2010 climatology^[3]. A large reduction in summer sea ice extent was observed in all Russian Arctic seas^[4]. In the Barents Sea, a significant decrease in sea ice also took place in the winter months^[5]. In March, the fraction of total ice extent that was made up of multiyear sea ice decreased from about 75% in the mid-1980s to 45% in 2011^[6]. Climate models indicate that the loss of Arctic sea ice enables navigability of moderately ice-strengthened ships through the Arctic Ocean via the North Pole in September by approximately the 2050s^[7–8].

Because of high year-to-year variability in Arctic sea ice spatial distribution, even today sea ice is the most significant obstacle for the use of the NEP. To assess the navigability of the NEP, the R/V *XUE LONG* icebreaker sailed from Bering Strait to the Norwegian Sea through the NEP at the end of July 2012. The voyage during the fifth Chinese National Arctic Research Expedition (5th CHINARE-Arctic, summer of 2012) made it the first Chinese vessel to use this sea route. In this study, remote sensing data from passive microwave and satellite-based altimeters were used to explore the seasonal changes in sea ice extent, concentration, thickness, and the open period of the NEP and the high-latitude sea route (HSR) north of the island groups in the eastern Arctic Ocean in 2007 and 2012. We also explored their anomalies relative to the 1981–2010 climatology. The data measured underway during the 5th CHINARE-Arctic were used to supplement the remote sensing data. Although sea ice conditions in the summers of 2007 and 2012 have been studied extensively^[3], few studies gave contributions from a shipping perspective. Thus, the results derived from this study can give support for the decision-making of stakeholders involved in the shipping industry, for example the ship owners, insurance agents and navigation authorities.

2 Materials and Methods

2.1 The 5th CHINARE-Arctic cruise and underway observations

XUE LONG sailed to point A in the Chukchi Sea on 22 July 2012 (Figure 1a, 68.0°N, 175.0°W) to start navigation through the NEP. The ship reached point B in the Norwegian Sea (75.1°N, 20.0°E) on 2 August. Here, we define the sea route from A to B (dashed red line in Figure 1a) as the standard NEP for the analysis. Our defined NEP is a major section of the conventional NEP, and includes all zonal sections of the Northern Sea Route (NSR), which is defined

in Russian Federation Law as a set of sea routes from Kara Gate to the Bering Strait (AMSA, 2009). However, in reality, the sea route is not fixed like our defined NEP, but should be adjusted according to sea ice distribution and bathymetry.

After fieldwork in the Nordic Seas, *XUE LONG* sailed to Point C (Figure 1a, 80.1°N, 10.0°E), north of Svalbard, on 24 August 2012, and started its eastward trip (solid gray line). In the north of the Laptev Sea, she started to navigate northward to carry out fieldwork in the central Arctic Ocean and reached the north most point (F) on 30 August. Finally, she sailed southward, reaching north of the Bering Strait (G, 68.1°N, 170.0°W) on 8 September. For the analysis, we define the HSR from C through E to D (dashed blue line in Figure 1a), excluding the track in the central Arctic Ocean from E through F to G. Comparable to the summer minimum sea ice extent (Figure 1a), the HSR stretches north of the island groups of Svalbard, Franz Joseph Land, Severnaya Zemlya, New Siberian and Wrangel. In the Laptev and East Siberian seas, the HSR stretches somewhat southward because of the bathymetric setting of the Arctic sea ice edge^[9]. The HSR can avoid most shallow waters along the coast, which may benefit deeper-draft vessels that wish to use the Arctic sea routes. A major objective in this study is to explore the seasonal and spatial changes in sea ice conditions through our defined NEP and HSR in 2007 and 2012.

During the navigation, routine observations were made every half an hour from the bridge of *XUE LONG* by trained observers, to document ice thickness, type, and concentration following the protocol compiled by the Antarctic Sea Ice Processes and Climate program (ASPeCt)^[10]. Sea ice concentration was estimated for a region surrounding the ship with a radius of about 2.5 km, which may be reduced to less than 0.5 km on foggy days. Sea ice thickness was estimated by comparing the scale of the stratigraphic cross-section of the overturned ice blocks alongside the hull of the vessel with that of a colored buoy with a diameter of 0.3 m suspended near the waterline. The accuracy of this method is about ± 0.1 m^[11]. This method could not be used to estimate the thickness of ice ridges that were almost broken when turned alongside the vessel. Thus, our observation of ice thickness was limited to level ice. Surface temperatures of water and sea ice along the tracks were measured by a downward-looking infrared thermometer, KT19.82 (Heitronics, Germany), with a spectral band of 8–14 μm and an accuracy of $\pm 0.2^\circ\text{C}$. The thermometer was mounted off the port side of *XUE LONG*, at a height of 40 m above the waterline and 1 m from the outermost surface of the ship's hull. Thus, we can avoid the ship's hull affecting the footprint of the sensor. The diameter of the measurement footprint was about 0.2 m above sea level. Upper seawater conductivity and temperature along the track was measured by a SBE 21 SEACAT Thermosalinograph (Sea-Bird Electronics, USA) fixed under *XUE LONG*. The accuracy of seawater conductivity and temperature measurements were ± 0.001 S·m⁻¹ and $\pm 0.01^\circ\text{C}$, respectively. The departure of upper seawater temperature from freezing point (DSF) can be calculated from these measurements. In

this study, we analyzed the data from underway observations along the NEP to supplement the remote sensing data.

2.2 Remote sensing data

Datasets of Nimbus-7 SMMR (Multichannel Microwave Radiometer, 1981–1986), DMSP SSM/I (Special Sensor Microwave/Imagers, 1987–2007) and SSMIS (Special Sensor Microwave Imager/Sounder, 2008–present) passive microwave data provide consistent data for sea ice concentration and extent^[12–13]. Monthly sea ice edges, defined by an ice concentration threshold of 15%, from July to October in 2007 and 2012 were used to quantify the seasonal changes in Arctic sea ice extent. Daily sea ice concentration from June to November, encompassing potentially the most

accessible period of the NEP^[7], were used to assess seasonal changes in ice conditions and to estimate the open period of the sea routes. Three ice-concentration thresholds of 75%, 50% and 15% were used to estimate the open period. These ice-concentration thresholds correspond to vessels of different ice-class levels. Most classification guidelines for icebreakers are scaled by ice thickness and ice type, e.g. the Polar Class^[14]. The dominant sea ice in the eastern Arctic Ocean is first-year ice^[6]. Year-round operation means that the corresponding sea ice concentration can reach a high level. Thus, on the basis of the general description of navigation requirements for icebreakers of different Polar Classes (Table 1), we can relate the ice-concentration thresholds of 75% to PC 4, 50% to PC 6 (e.g. *XUE LONG*), and 15% to common open-water vessels (e.g. the *Yongsheng*).

Table 1 General description of Polar Class^[14]

| Classification | Navigational conditions | Minimum required level of icebreaking capability/m |
|----------------|--|--|
| PC 1 | Year-round operation in all Arctic ice-covered waters | 3.0 |
| PC 2 | Year-round operation in moderate multiyear ice conditions | 2.4 |
| PC 3 | Year-round operation in second-year ice that may include multiyear ice inclusions | 1.8 |
| PC 4 | Year-round operation in thick first-year ice that may include old ice inclusions | 1.3 |
| PC 5 | Year-round operation in medium first-year ice that may include old ice inclusions | 1.0 |
| PC 6 | Summer/autumn operation in medium first-year ice that may include old ice inclusions | 0.7 |
| PC 7 | Summer/autumn operation in thin first-year ice that may include old ice inclusions | 0.5 |

Sea ice thickness, derived from the ICESat (Ice, Cloud, and land Elevation satellite), is available from 2003 to 2008^[15]. Each autumn and winter, the ICESat campaign over the Arctic Ocean covers a 33-day period from roughly mid-October to mid-November (2003–2007) and from late February to late March (2004–2008). The data are archived as composite values of October–November for autumn and February–March for winter, with the exception of the 2007 winter, which was March–April. The data for the section 20°–104°E of the NEP are unavailable because of the dome limitations of ICESat measurements. Sea ice thickness derived from the CryoSat-2 is available from 2010 to present^[16]. These data are compiled monthly by the CryoSat-2 level-2 processor developed at the Alfred Wegener Institute^[17]. To compare with the ICESat product, we calculated 2-month averages for March–April 2012 using the CryoSat-2 data. Seasonal changes in sea ice thickness cannot be ascertained for 2007 because of the temporal limitations of ICESat campaigns. For the Arctic marginal ice zone in summer, the error of the CryoSat-2 product cannot be ignored^[17]. Therefore, only the data from February to May were used to ascertain seasonal changes in sea ice thickness for 2012.

Along the sea routes, the test points were defined at 0.25 longitudinal gaps. In total, 661 and 721 test points were defined through the NEP and HSR, respectively. All the remote sensing data were bilinearly interpolated to the test points before analyses. We defined the boundaries of the

Chukchi, East Siberian, Laptev, Kara and Barents sections along the sea routes at approximately 179°E, 142°E, 103°E, and 67°E, respectively.

3 Results

3.1 Sea ice edge

As shown in Figure 1 and Table 2, monthly anomalies of the latitudes of sea ice edge were almost positive (more northerly) for all Eurasian subsections from July to October in 2007 and 2012, except for those in July and October of 2012 in the Chukchi Sea. This implies a distinct sea ice decline in both summers. In September, the anomalies of the Arctic sea ice edge were significantly larger than other months for all subsections. This corroborates the results obtained from the trend analysis of sea ice extent, which also identified September as the month when the most significant decrease occurred for the whole Arctic Ocean and the Pacific sector of the Arctic^[18–19]. In September, the sea ice decline in the Chukchi and East Siberian seas was larger than in other subsections, which confirmed that the most substantial loss in summer Arctic sea ice occurred in the Pacific sector^[20]. The changes in summer sea ice in this sector dominated the long-term changes and year-to-year variations over the whole Arctic Ocean^[21].

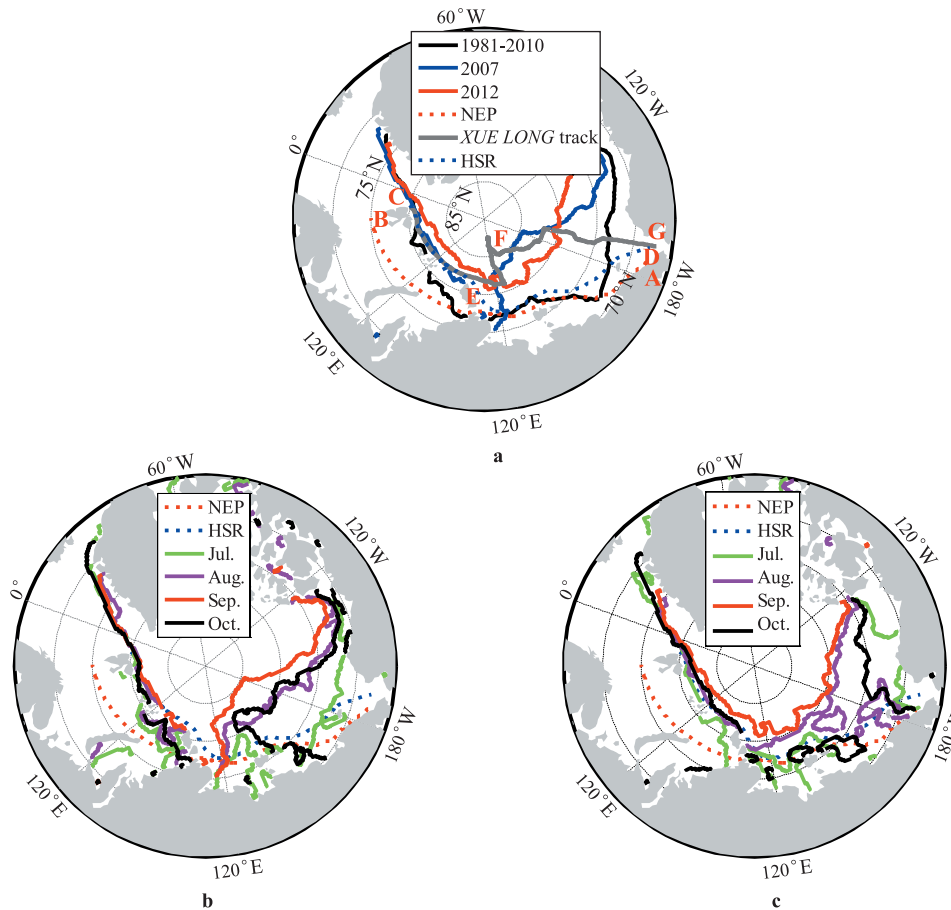


Figure 1 September Arctic sea ice edges of the 1981–2010 climatology, and 2007 and 2012. Also shown are the *XUE LONG*'s tracks along the NEP (A to B) and in the high latitudes (from C through E and F to G), and our defined HSR (from C through E to D) (a); monthly Arctic sea ice edge from July to October in 2007, also shown are the NEP and HSR (b); monthly Arctic sea ice edge from July to October in 2012, also shown are the NEP and HSR (c).

Table 2 Average northern latitudes of the monthly Arctic sea ice edge for the Eurasian subsections from July to October in 2007 and 2012, with their corresponding anomalies in parentheses relative to the 1981–2010 climatology (positive values correspond to a more northerly ice edge)

| Year | Month | Chukchi / (°) | East Siberian / (°) | Laptev / (°) | Kara / (°) | Barents / (°) | Year | Month | Chukchi / (°) | East Siberian / (°) | Laptev / (°) | Kara / (°) | Barents / (°) |
|------|-----------|----------------|---------------------|---------------|---------------|---------------|------|-----------|----------------|---------------------|---------------|---------------|---------------|
| 2007 | July | 71.8 (2.1) | 73.2 (2.8) | 75.7 (2.1) | 77.4 (2.8) | 79.7 (3.8) | 2012 | July | 69.3 (-0.4) | 75.1 (4.6) | 76.6 (3.0) | 79.2 (4.6) | 80.9 (5.0) |
| | August | 77.5 (5.4) | 80.2 (8.0) | 78.3 (1.8) | 79.3 (3.7) | 80.5 (0.7) | | August | 72.8 (0.7) | 76.1 (3.8) | 79.4 (2.9) | 81.8 (6.1) | 81.6 (1.8) |
| | September | 83.4 (10.5) | 84.4 (11.1) | 78.7 (1.5) | 81.2 (4.1) | 81.6 (0.9) | | September | 79.9 (6.9) | 80.8 (7.5) | 81.3 (4.1) | 83.3 (6.2) | 83.1 (2.5) |
| | October | 79.1 (8.0) | 72.7 (2.3) | 74.1 (0.5) | 76.9 (2.9) | 80.7 (1.8) | | October | 70.9 (-0.2) | 73.8 (3.5) | 76.9 (3.3) | 77.4 (3.4) | 81.6 (2.7) |

Comparing the 2 years shows that sea ice declines in the Chukchi and East Siberian seas were more significant in 2007 than in 2012. Contrarily, there were more significant declines in other subsections in 2012. The anomalous loss of sea ice in the Pacific sector during the summer of 2007

distinctly delayed refreezing in autumn. Therefore, the marginal seas north of eastern Siberia were still open in October (Figure 1b). In July 2007, there was a distinct sea ice tongue reaching relatively low latitudes near the northeast coast of the Taimyr Peninsula (the northernmost extremity of

the Eurasian landmass). This ice tongue remained through the entire summer of 2007 and prevented the opening of the NEP (Figure 2b). Consequently, the decline of sea ice in the Laptev Sea was much smaller in the summer of 2007 than in 2012. Southerly winds from Russia blew most of the landfast sea ice along the Laptev shore to the north during the 2011–2012 winter. This resulted in relatively thin sea ice, generally less than 0.5 m, by April 2012, as identified by SMOS (Soil Moisture and Ocean Salinity) data^[22], which accelerated the summer opening of the sea route. In July 2012, most parts of the Arctic sea ice edge reached the coasts of East Siberia and Alaska. In August 2012, some sizeable sea ice segments were sheared from the main Arctic pack ice zone into the Chukchi and East Siberia seas. However, these sea ice segments subsequently melted. Thus, by September 2012, the ice edge in the Chukchi and East Siberian seas shrank remarkably, and reached the second highest latitudes since 1979, being just below the 2007 edge. For the Kara and Barents sections, the sea ice edge moved from the coasts of Svalbard, Franz Joseph Land and Severnaya Zemlya northward, about 2 latitudinal degrees by late August 2012. This resulted in the opening of the sea route north of the islands. Consequently, *XUE LONG* could navigate through without any pilot vessel.

3.2 Sea ice concentration and open period

Figure 2 shows sea ice concentration along the NEP and HSR from 1 June to 30 November in 2007 and 2012. Because of the aforementioned ice tongue reaching the Taimyr Peninsula, both the NEP and HSR were not open completely throughout the entire 2007 summer. The NEP was ice free by mid-July 2007, except the section 93°–124°E, which spans the western Laptev Sea, the Vilkitskiy Strait and the eastern Kara Sea. This ice belt had shrunk and ice conditions gradually weakened as midsummer approached. By the end of August 2007, the ice-blocked section of the NEP shrank to 100°–124°E and the ice concentration decreased to about 50%. Excluding this section, sea ice conditions in 2007 were weaker than or comparable to the 1981–2010 climatology from mid-July to late October. The Chukchi section of the NEP was ice free from mid-June to mid-November in 2007, which was about 2.5 months longer than in 2012. The East Siberian section of NEP was ice free from mid-July to late October, which was about 25 d longer than that in 2012. Thus, the eastern NEP section was more accessible in 2007 because of the remarkable decline in Arctic sea ice in the Pacific sector. In 2012, some fragmentary floes appeared in

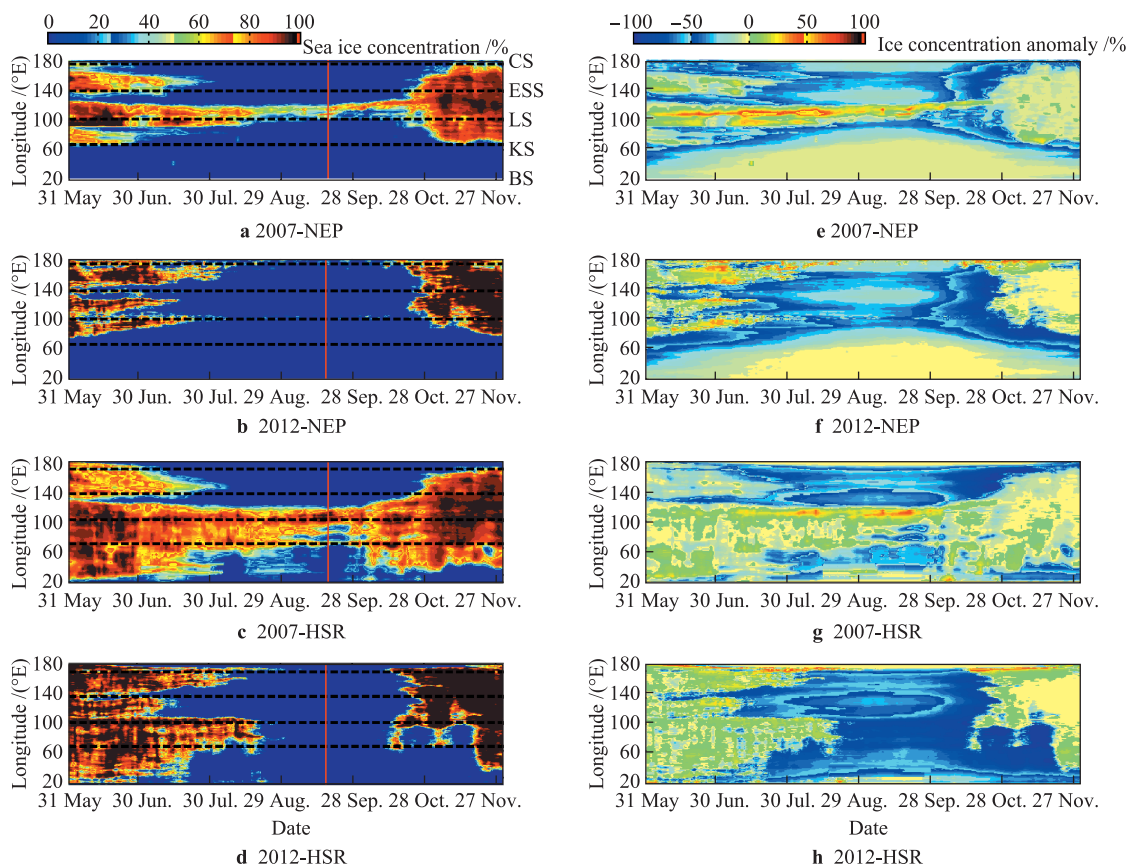


Figure 2 Sea ice concentration along the NEP and the HSR from 1 June to 30 November in 2007 and 2012 (a–d), and their corresponding anomalies relative to the 1981–2010 climatology (e–h). The red lines in panels a–d denote the dates when Arctic sea ice extent reached its annual minimum, and dashed black lines separate the subsections of the Chukchi (CS), East Siberian (ESS), Laptev (LS), Kara (KS) and Barents (BS).

the Chukchi section and Vilkitskiy Strait from mid-August to mid-October. However, at that time, the ice concentration was almost less than 30%. Excluding these two sections, the sea route was completely ice free. Thus, the NEP was accessible for more than 3 months during the 2012 summer, even for common open-water vessels. The Barents section of the NEP was ice free from June to November in both years. The winter data on ice concentration further validated year-round ice-free conditions in this section for both years, which implies an increasing “Atlantification” of the Barents Sea from a shipping perspective. This can be attributed to the more pronounced winter ice retreat occurring in this sea, compared with other regions of the Arctic Ocean^[5]. Seasonally, the most negative ice-concentration anomaly occurred in the early autumn for both years, when the open water started to refreeze, indicating a delay in refreezing. The secondary anomaly occurred in July, which can be related to the earlier onset of the ice melt season.

In 2007, the ice belt blocking the HSR was more extensive than for the NEP. At the time when Arctic sea ice extent reached its annual minimum, this ice belt still spread 65°–126°E, through the HSR. Compared with the 2007 HSR, the 2012 HSR had: (a) a completely ice-free period lasted about 45 d, (b) sea ice conditions that were relatively heavy in the Chukchi and East Siberian sections, with an ice-free period about one to two months shorter, and (c) sea

ice conditions that were relatively weak in other sections, especially for the Barents section, because of the ice edge moving northwards about 2 latitudinal degrees from Svalbard, Franz Joseph Land and Severnaya Zemlya by September 2012.

Ship-based underway measurements show that, by late July 2012, the heaviest sea ice conditions occurred in the eastern part of the East Siberian Sea and the De Long Strait (155°–180°E), where sea ice concentration ranged from 50% to 90%. Surface temperatures indicate the melt state of ice/snow surface. The melt point of the sea ice surface in summer may approach 0°C because of the desalination of the upper ice layer^[11]. Along the NEP, surface temperatures of sea ice ranged from -1.2°C to 0°C, suggesting a melting ice surface (Figure 3a). Only in rare cases, surface temperatures of ice region can rise above 0°C and peak at 2.0°C because of puddling over the ice surface. The formation of a melt pond can remarkably accelerate ice surface melt because of its relatively low albedo. For open water, surface temperatures ranged from 0°C to 10.0°C. Generally, the region with higher ice concentration might have a relatively cold surface temperature, and vice versa (Figures 3a and 3c). However, the Chukchi section had a local maximum reaching 8.5°C, although there was 20%–50% ice concentration. This can be attributed to this region being so close to the Bering Strait that it can obtain more heat advected from the Pacific Ocean. The

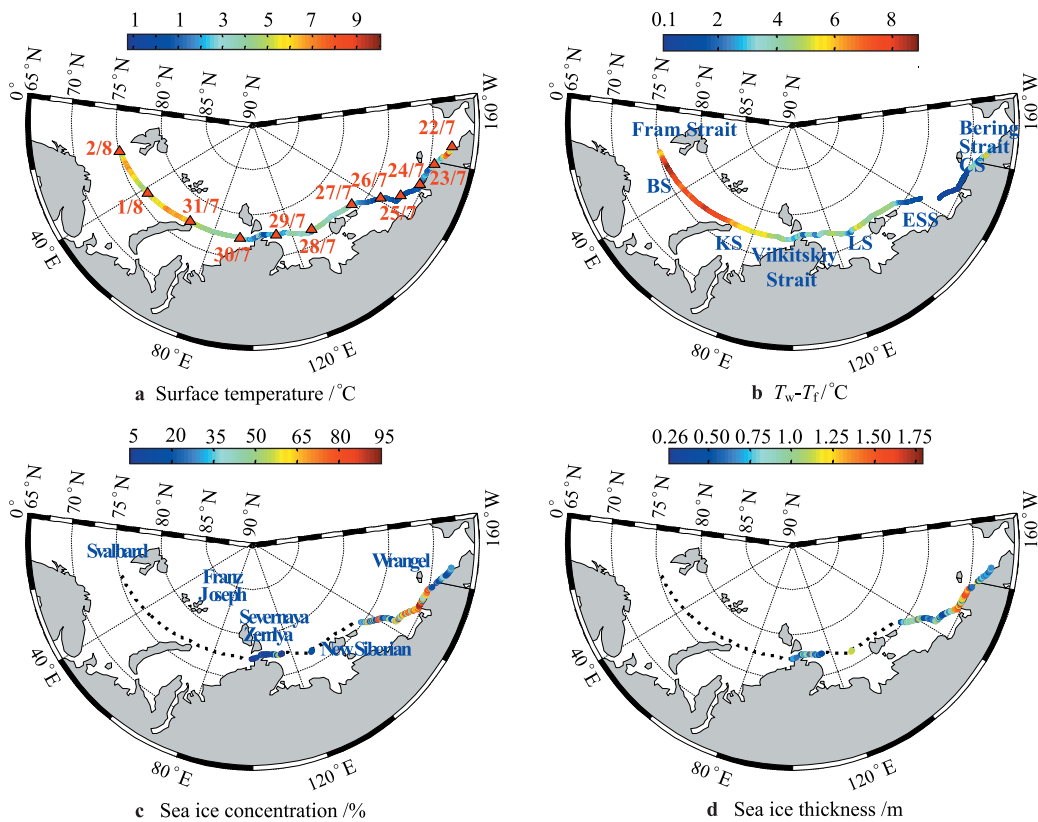


Figure 3 Underway observed surface temperature of open water or sea ice (a), the departure of the upper seawater temperature (T_w) from freezing point (T_f) (b), sea ice concentration and thickness (c–d) along the NEP from 22 July to 2 August 2012. Also shown are the daily locations of *XUE LONG* (triangles) in panel A and the ice-free parts of the NEP (black dot line) in panels c–d.

De Long and Vilkitskiy Straits are two of the most crucial points for spatial changes in surface temperature. Their relatively shallow waters can reject most of the heat advected from the Pacific and Atlantic Oceans. Thus, the section between the two straits generally has relatively short ice-free period. The DSF can indicate the oceanic heat under the ice to a high degree^[23–24]. The spatial changes in this variable had a similar pattern to the surface temperature (Figure 3b). Both variables had local minima in the eastern part of the East Siberian section. The DSF was close to zero in this region, which implied that oceanic heat was very trivial. The relatively cold ice surface and under-ice seawater in this region can effectively prevent ice melt from both the surface and bottom. Thus, most sea ice in this region remained until early August 2012 (Figure 2b).

As expected, using a smaller ice-concentration threshold gives a shorter open period, especially for regions with heavy ice condition (Figure 4). For example, in the East Siberian section of the NEP (143°–179°E), the spatial average open periods were 88, 104 and 120 d in 2012, corresponding to the ice-concentration thresholds of 15%, 50% and 75%, respectively. In contrast, for regions with relatively slight ice condition, this discrepancy might be reduced. For example in the Kara section of the NEP (67°–103°E), the corresponding open periods were 143, 150 and 159 d, respectively. Thus, using a higher ice-class of vessel can effectively extend the navigable period, especially for regions covered by heavy sea ice.

Relative to the 1981–2010 climatology, along the NEP,

the negative anomalies of the open period occurred around the Vilkitskiy Strait and the eastern Laptev section in 2007, and in the Chukchi section in 2012, both because of the relatively heavy ice conditions. In the Barents section, these anomalies approached zero, implying that this region was accessible from June to November for most years from 1981 to 2010. Along the NEP, the highest positive anomalies of the open period occurred in the Chukchi section and the eastern part of the East Siberian section (160°–185°E) in 2007, because of the remarkable decline in Arctic sea ice in the Pacific sector. The highest anomaly in 2012 occurred in the Kara section, with an open period as defined by 50% ice concentration that was 86 d longer than the 1981–2010 climatology. This can be attributed mainly to changes in the preconditioning of ice prior to the melt season. In the winter and spring months of 2011–2012, the ice extent in the Barents and Kara seas were well below the 1981–2010 climatology, because of relatively warm air temperature and anomaly enhanced southerly winds. News and analysis on Arctic sea ice released by the National Snow and Ice Data Center showed that surface air temperatures remained above normal by 4°C to 6°C in the Barents and Kara seas during the winter months of 2011–2012 (<http://nsidc.org/arcticseaicenews/2012/04/>).

Along the HSR, the 60°–120°E section was almost inaccessible in 2007, based on the ice-concentration threshold of 15%. Even using the 75% threshold, the open period of this section was almost less than 50 d. Thus, we can declare that the sea route from north of Franz Joseph Land to north of Severnaya Zemlya was worthless for shipping even using a

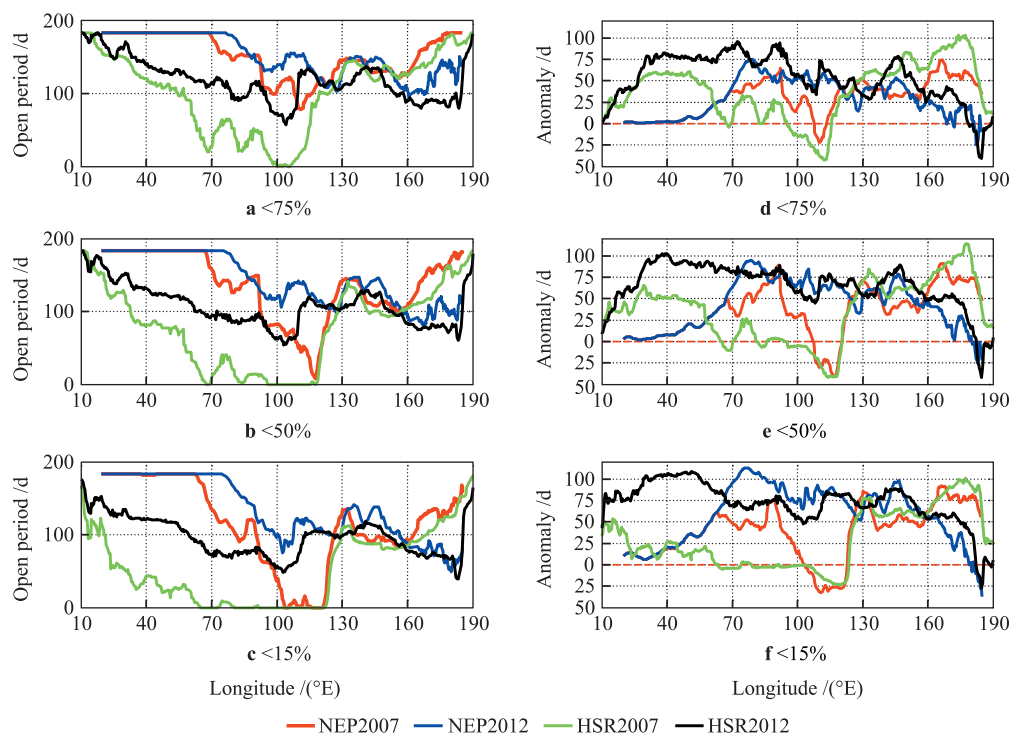


Figure 4 Open period defined by ice-concentration thresholds of 75%, 50% and 15% along the NEP and the HSR from 1 June to 30 November in 2007 and 2012 (a–c), and their corresponding anomalies relative to the 1981–2010 climatology (d–f).

vessel of PC 4 in the 2007 summer. However, the open period of this section increased to longer than 50 d in the 2012 summer, even using the 15% threshold, which effectively enhanced its potential navigability. Both satellite-based and ship-based observations show that this section became completely ice free by the end of August 2012. Except for this section, the HSR was open in both years. Relative to the 1981–2010 climatology, the highest positive anomaly along the HSR in 2012 occurred in the Barents and Kara sections, because these sections were almost inaccessible in most previous years.

3.3 Sea ice thickness

From Figures 5 and 6, we found that there was a mass of thick sea ice (>2.5 m) accumulating along the East Siberia coast (165°–185°E) from February to May 2012. Thus, the survival of thick sea ice from winter effectively hindered the summer opening of the Chukchi section and the eastern part of the East Siberian section for both the NEP and HSR in 2012. Ship-based observations in late July 2012 also showed that there were still some level floes thicker than 1.5 m in the eastern part of the NEP East Siberian section (Figure 3d). Except for this section, the March–April sea ice along the NEP and HSR in 2012 was remarkably thinner than in 2007. Most parts of the western section of

10°–50°E along the HSR were ice free, even in the winter months of 2011–2012, which could give an advantageous precondition for summer opening. A remarkable southward extension by about 1.5 latitudinal degrees of pack ice edge occurred north of Svalbard during April 2012 because of enhanced northerly winds in the first half of the month. This significantly increased sea ice thickness along the 10°–50°E section of the HSR (Figure 6a). However, the ice edge shrank northwards again during mid-May. Thus, sea ice thickness decreased again in May 2012. Comparison of the frequency distributions of sea ice thickness between the two years shows that: (a) most sea ice thicker than 2.0 m in 2007 was replaced by ice thinner than 1.25 m in 2012, and (b) the mode peak moves from 1.5–2.0 m in 2007 to 1.25–1.75 m in 2012. The long tail for ice thicker than 2.5 m in 2012 can be related to the thick ice spreading along the East Siberian coast.

4 Discussions

The high positive polarity of the Arctic Oscillation (AO), associated with a stronger clockwise Beaufort Gyre, effectively restricted the accessibility of the eastern part of the NEP, by advecting more thick ice from the north Canadian Arctic Archipelago to the coast of East Siberia. From November through to the first half of January in the 2011–2012 winter, the AO was in a generally positive phase.

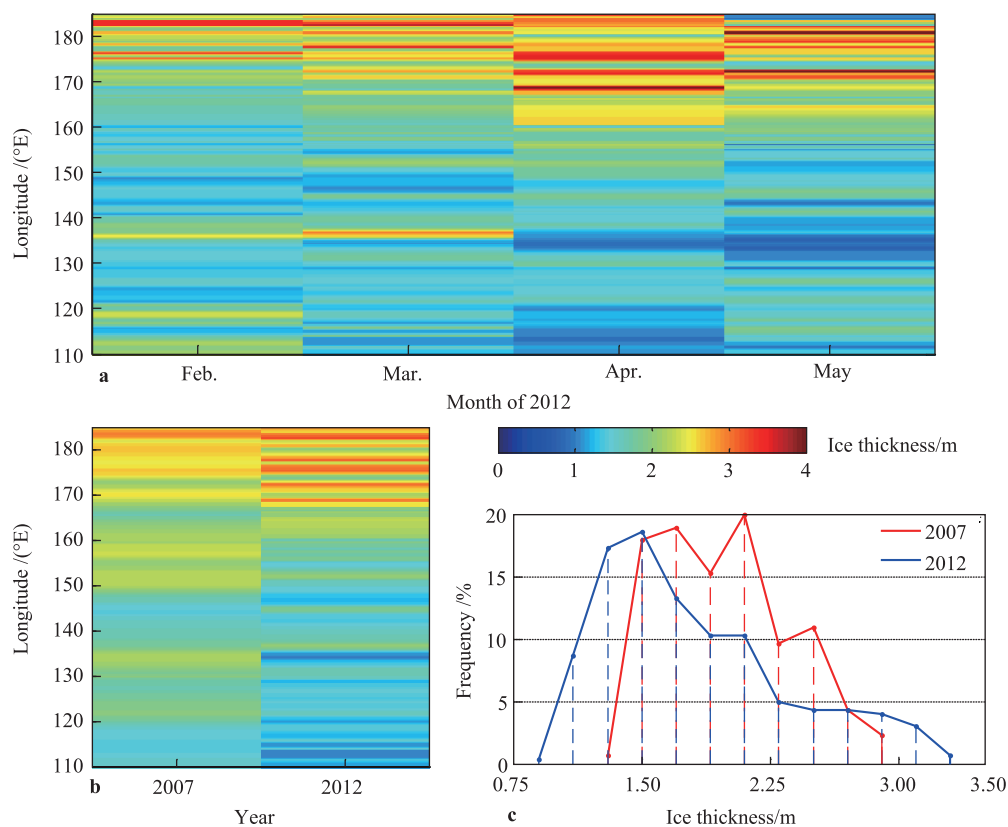


Figure 5 Monthly sea ice thickness derived from CryoSat-2 along the NEP from February to May in 2012 (a). March–April ice thickness in 2007 (from ICESat) and 2012 (from CryoSat-2), and their corresponding frequency distributions (b–c).

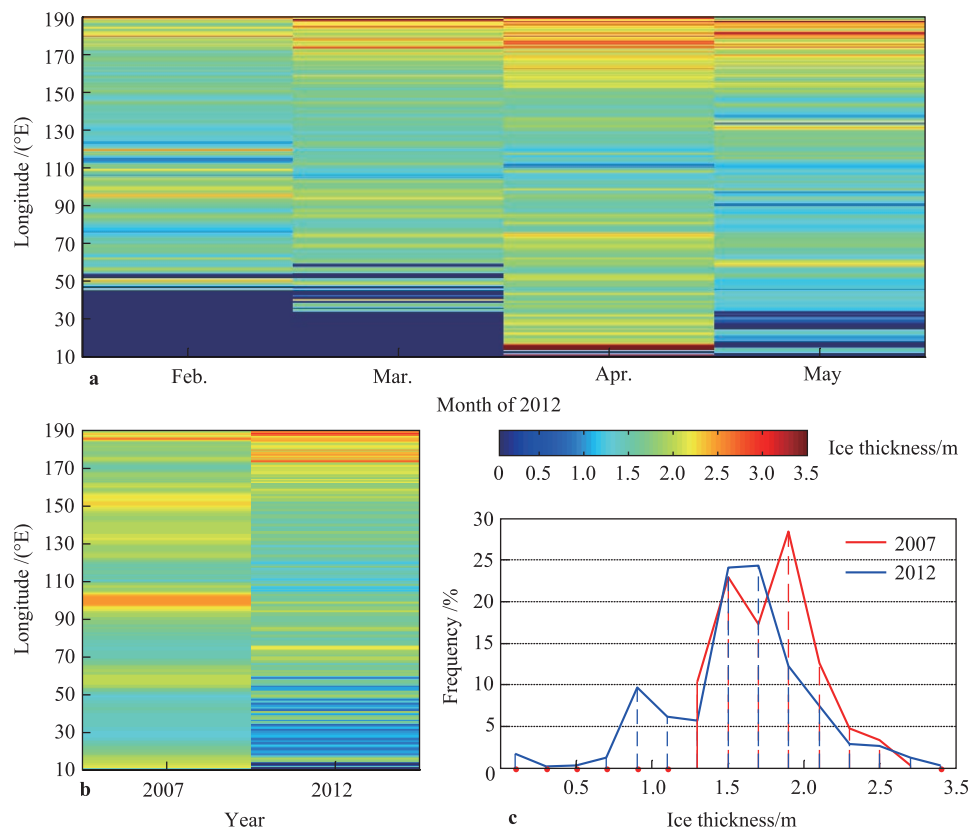


Figure 6 Monthly sea ice thickness derived from CryoSat-2 along the HSR from February to May in 2012 (a). March–April ice thickness in 2007 (from ICESat) and 2012 (from CryoSat-2), and their corresponding frequency distributions (b–c).

Thus, a mass of thick multiyear sea ice was advected to and accumulated along the coast of East Siberia (Figures 5 and 6). This differed from conditions in July 2007^[25]. In the 2011–2012 winter, the sea ice extent in the Pacific sector reached unusually far south and sea ice concentration was almost 100% in the Chukchi Sea. Thus, the thick ice could not be advected westwards beyond the coast of East Siberia. The unusual easterly winds prevailing in July 2007 advected the thick ice further westwards into the eastern Laptev Sea and piled up east of the Taimyr Peninsula and Severnaya Zemlya islands. Since the ice melt season has started by July 2007, there were a mass of leads appeared among the floes or between sea ice and the coast, which acted as corridors for sea-ice advection.

The strengthened transpolar drift in the 2007 summer^[25], mainly stimulated by the high positive polarity of the Arctic Dipole Anomaly^[26], resulted in unusual Arctic sea ice decline in the Pacific sector, and furthermore a relatively long summer opening in the East Siberian and Chukchi sections of the NEP. The atmospheric circulation pattern in the 2012 summer did not favor Arctic sea ice outflow. However, in early August 2012, a major storm moved into the central Arctic from Siberia. By 6 August 2012, this storm reached its lowest central pressure at approximately 81°N and 165°W^[27]. This storm lasted about two weeks and sheared off about 0.4×10^6 km² sea ice from the main Arctic pack ice zone, to

the north of the Bering Strait^[3]. Most sheared-off sea ice accumulated around the Wrangel Islands and East Siberian coast (Figure 1c), which obstructed the opening of the NEP in the first half of August. However, the sheared-off ice melted rapidly because of exposure to warm liquid water and wave action^[3], which favored the decline of Arctic sea ice extent in the Pacific sector and the opening of sea routes during late August 2012.

5 Conclusions

From the above data analysis, we find that the predominant factors determining the opening of the NEP include the preconditions of sea ice prior to the melt season, e.g. sea ice thickness and edge location, atmospheric circulation pattern through the year, and storms occurring in the melt season. The thinner sea ice in 2012, especially for the western part, can partly contribute to the longer summer opening relative to 2007. However, the sea ice shearing from the Arctic pack ice during a great storm in early August, and the thick ice surviving from winter, delayed the summer opening of the eastern parts of the sea routes in 2012.

Defined by the ice concentration threshold of 50%, the open period of the entire NEP was 82 d in 2012, while this open period was only 8 d in 2007 because of the blocking of an ice tongue extending from the Arctic pack ice zone

to the Taimyr Peninsula. Using the same definition, the open period of the HSR was 55 d in 2012. Furthermore, the completely ice-free period of the HSR reached 47 d in 2012 summer. It means that *XUE LONG*, which can sail through waters covered by 50% sea ice at a speed of about 5–8 knots, could use the HSR for more than 1.5 months during the 2012 summer. A vessel without any icebreaking capability could use this sea route for more than one month. Using the HSR for shipping avoids the shallow waters along the Russian coast and therefore benefits deeper-draft vessels. The lengthening of the HSR summer opening can be considered as an expansion of the NEP from the Russian shelf to higher latitudes, which can also restrain the control of Russia over the NEP. Importantly, it can avoid the Vilkitskiy Strait, which is generally claimed as internal waters by Russia. However, sea ice conditions along the HSR have still been relatively heavy and shown large year-to-year variability in recent years. For example in the Kara section, where the sea ice was heaviest along the HSR, the open period, defined by 50% ice concentration, ranged from 12 to 85 d from 2007 to 2012. Thus, this sea route cannot currently be recommended for merchant shipping.

Acknowledgements This work was supported financially by the grants from the National Natural Science Foundation of China (Grant nos. 41106160, 41476170), the Chinese Polar Environment Comprehensive Investigation and Assessment Programs (Grant nos. CHINARE2014-04-03, CHINARE 2014-04-04, CHINARE2014-03-01), and the Ocean Public Welfare Scientific Research Project of China (Grant no. 201205007).

References

- 1 AMSA. Arctic Marine Shipping Assessment 2009 report. Protection of the Arctic Marine Environment working group (PAME) of the Arctic Council, Akureyri. <http://www.pame.is/amsa/amsa-2009-report>, 2009.
- 2 Stephenson S R, Brigham L W, Smith L C. Marine accessibility along Russia's Northern Sea Route. *Polar Geography*, 2014, 37(2): 111–113, doi: 10.1080/1088937X.2013.845859.
- 3 Parkinson C L, Comiso J C. On the 2012 record low Arctic sea ice cover: Combined impact of preconditioning and an August storm. *Geophysical Research Letters*, 2013, 40(7): 1356–1361, doi: 10.1002/grl.50349.
- 4 Mahoney A R, Barry R G, Smolyanitsky V, et al. Observed sea ice extent in the Russian Arctic, 1933–2006. *Journal of Geophysical Research*, 2008, 113(C11005), doi: 10.1029/2008JC004830.
- 5 Rodrigues J. The rapid decline of the sea ice in the Russian Arctic. *Cold Regions Science and Technology*, 2008, 54(2): 124–142.
- 6 Maslanik J, Stroeve J, Fowler C, et al. Distribution and trends in Arctic sea ice age through spring 2011. *Geophysical Research Letters*, 2011, 38(L13502), doi: 10.1029/2011GL047735.
- 7 Stephenson S R, Smith L C, Brigham L W, et al. Projected 21st-century changes to Arctic marine access. *Climatic Change*, 2013, 118(3–4): 885–899.
- 8 Smith L C, Stephenson S R. New trans-Arctic shipping routes navigable by midcentury. *Proceedings of the National Academy of Sciences of the United States of America*, 2013, 110(13): 1191–1195.
- 9 Nghiem S V, Clemente-Colón P, Rigorc I G, et al. Seafloor control on sea ice. *Deep Sea Research II*, 2012, 77–80: 52–61.
- 10 Worby A P, Geiger C A, Paget M J, et al. Thickness distribution of Antarctic sea ice. *Journal of Geophysical Research*, 2008, 113(C05S92), doi: 10.1029/2007JC004254.
- 11 Lei R B, Li Z J, Li N, et al. Crucial physical characteristics of sea ice in the Arctic section of 143°W–180°W during August and early September 2008. *Acta Oceanologica Sinica*, 2012, 31(4): 65–75.
- 12 Cavalieri D J, Parkinson C L, Gloersen P, et al. *Sea Ice Concentrations from Nimbus-7 SMMR and DMSP SSM/I-SSMIS Passive Microwave Data*. Boulder, Colorado USA: NASA DAAC at the National Snow and Ice Data Center, 1996.
- 13 Fetterer F, Knowles K, Meier W, et al. *Sea Ice Index*. Boulder, Colorado USA: National Snow and Ice Data Center, 2002.
- 14 IACS, 2011. Requirements concerning polar class. International Association of Classification Societies, London. http://www.iacs.org.uk/document/public/publications/unified_requirements/pdf/ur_i_pdf410.pdf.
- 15 Kwok R, Cunningham G F. ICESat over Arctic sea ice: Estimation of snow depth and ice thickness. *Journal of Geophysical Research*, 2008, 113(C08010), doi: 10.1029/2008JC004753.
- 16 Laxon S W, Giles K A, Ridout A L, et al. CryoSat-2 estimates of Arctic sea ice thickness and volume. *Geophysical Research Letters*, 2013, 40(4): 732–737, doi: 10.1002/grl.50193.
- 17 Hendricks S, Ricker R, Helm V. AWI. CryoSat-2 sea ice thickness data product, v1.0. 2013, Helmholtz Centre, Alfred Wegener Institute for Polar and Marine Research, Bremerhaven, Germany. <http://www.meereisportal.de>.
- 18 Stroeve J C, Kattsov V, Barrett A, et al. Trends in Arctic sea ice extent from CMIP5, CMIP3 and observations. *Geophysical Research Letters*, 2012, 39(L16502), doi: 10.1029/2012GL052676.
- 19 Su J, Wei J F, Li X, et al. Sea ice area inter-annual variability in the Pacific sector of the Arctic and its correlations with oceanographic and atmospheric main patterns // *Proceedings of the 21 International Offshore and Polar Engineering Conference*. Hawaii, USA, 2011: 19–24.
- 20 Stroeve J C, Serreze M C, Holland M M, et al. The Arctic's rapidly shrinking sea ice cover: a research synthesis. *Climatic Change*, 2012, 110(3–4): 1005–1027.
- 21 Ogi M, Wallace J M. Summer minimum Arctic sea ice extent and the associated summer atmospheric circulation. *Geophysical Research Letters*, 2007, 34(L12705), doi: 10.1029/2007GL029897.
- 22 Tian-Kunze X, Kaleschke L, Maass N. Updated current year. SMOS Daily sea ice thickness. 2013, ICDC, <http://icdc.zmaw.de>, University of Hamburg, Germany, Digital media.
- 23 McPhee M G, Morison J H, Nilsen F. Revisiting heat and salt exchange at the ice-ocean interface: Ocean flux and modeling considerations. *Journal of Geophysical Research*, 2008, 113(C06014), doi: 10.1029/2007JC004383.
- 24 Lei R B, Li N, Heil P, et al. Multiyear sea-ice thermal regimes and oceanic heat flux derived from an ice mass balance buoy in the Arctic Ocean. *Journal of Geophysical Research*, 2014, 119(1): 537–547, doi: 10.1002/2012JC008731.
- 25 Zhang J L, Lindsay R, Steele M, et al. What drove the dramatic retreat of arctic sea ice during summer 2007? *Geophysical Research Letters*, 2008, 35(L11505), doi: 10.1029/2008GL034005.
- 26 Wang J, Zhang J L, Watanabe E, et al. Is the Dipole Anomaly a major driver to record lows in the Arctic summer sea ice extent? *Geophysical Research Letters*, 2009, 36(L05706), doi: 10.1029/2008GL036706.
- 27 Simmonds I, Rudeva I. The great Arctic cyclone of August 2012. *Geophysical Research Letters*, 2012, 39(L23709), doi: 10.1029/2012GL054259.